Pattern Regularity as a Visual Key

Dmitry Chetverikov
Image and Pattern Analysis Group
Computer and Automation Research Institute
Budapest, Kende u.13-17, H-1111 HUNGARY
csetverikov@sztaki.hu

Abstract

Regular structures, flat and non-flat, are perceived as regular in a wide range of viewing angles and under varying illumination. In this papers, we exploit this simple observation and develop an invariant measure of pattern regularity. The measure is the maximum of the regularity values obtained for different directions within the pattern. We demonstrate that the regularity feature introduced is reasonably stable under weak perspective of real non-flat structures. The feature is consistent with human perception of texture regularity. It is used for regularity-based image filtering. Examples of invariant detection of periodic structures are shown. Finally, structural defects in regular textures are detected as locations of low regularity.

1 Introduction

Figure 1 shows a set of patterns which look different but have much in common. They are different views of the same three-dimensional, periodic structure indicated by a box in a RADIUS [10] model board image shown in figure 5.

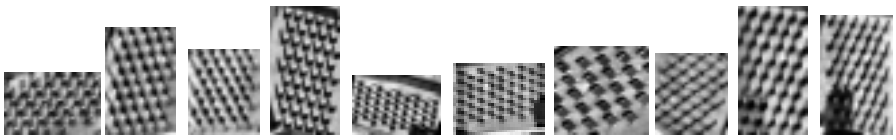

Figure 1: Different views of a non-flat regular structure.

Pattern	1	2	3	4	5	6	7	8	9	10
Value	0.78	0.89	0.88	0.87	0.90	0.85	0.84	0.86	0.83	0.85

Table 1: The regularity values of the patterns shown in figure 1.

The numbers in table 1 are the values of the proposed regularity measure computed for these patterns. The range is $[0, 1]$, with 1 being perfect periodicity. The regularity values show surprising stability, compared to the significant changes in the appearance

BMVC 1998 doi:10.5244/C.12.3

of the viewed object. This is consistent with the fact that a regular structure is perceived by humans as regular under a wide range of affine transformations. To a certain extent, this is valid even for non-flat structures and changing illumination. Thus, a properly defined measure of pattern regularity can serve as a highly invariant, perceptually motivated feature. In this paper, we propose such a feature and show examples of its application.

Previous attempts to evaluate pattern regularity were mostly aimed at textures viewed as planar patterns under two-dimensional shift, rotation and zoom. Our current approach is related to the early studies by Zucker and Terzopoulos [13] and Chetverikov [1]. The former applies the chi-test to the co-occurrence matrix and searches for those displacement vectors that coincide with the periodicity vectors. However, no regularity measure is defined. The latter uses a gray-level difference histogram (GLDH) feature and proposes a model-based regularity measure for a given direction.

In both [13] and [1], the conventional, raster-based pairwise spatial relation between the pixels was used. Later, we showed [5] that this relation is unsuitable for precise analysis of anisotropy and regularity at arbitrary orientations. The extended co-occurrence was proposed to decouple the magnitude and the angle of the displacement vector.

Rao and Lohse [11] demonstrated that regularity plays an important role in human texture perception. Tamura et.al. [12] proposed a set of texture features, including regularity, that correspond to human perception. Their regularity measure is defined via the spatial variation of four other features, such as coarseness and directionality. However, the experimental study in [12] indicated poor correlation between the proposed computational measure and the visually perceived regularity.

D'Astous and Jernigan [6] approach texture regularity using the characteristic frequencies of the power spectrum. A similar, power spectrum based view of regularity (periodicity) is adopted in the recent work by Liu and Picard [8].

There are different components of regularity, including regularities in the spatial layout and in the intensity distribution of the elements comprising the pattern [3]. A detailed analysis of regularity should therefore try to characterize these components separately, which we plan to do in the future. In our current study, two partial measures are combined into an overall measure.

The main contributions of this paper are a new definition of pattern regularity and an implementation of this feature in a fast and flexible regularity filter. Emphasizing the invariance of regularity, we make an attempt to extend the scope of this visual feature to non-flat patterns. In the rest of the paper, we introduce the maximal regularity feature and show examples of its application to some problems of computer vision, including classification of texture patterns according to regularity, search for periodic structures of arbitrary orientation, and detection of structural defects.

2 The maximal regularity measure

2.1 The $MEAN$ feature of the EGLDH

Our definition of regularity is based on the *extended graylevel difference histogram* EGLDH [5, 3]. Consider a $M \times N$ pixel size digital image $I(m, n)$ and a spacing vector $\vec{d} = (\alpha, d)$, with α being the orientation, d the magnitude of the vector. The histogram is computed by scanning the image by $\vec{d}$ and counting the occurrences of the absolute graylevel differences between the two points connected by the vector. The origin of $\vec{d}$ moves on the

image raster, while the end of the vector points at a non-integer location. When the origin is in the pixel (m, n), $\vec{d}$ points at the location (x, y) given by

$$\begin{aligned} x &= n + d\cos\alpha \\ y &= m - d\sin\alpha \end{aligned} \tag{1}$$

The intensity $I(x, y)$ is obtained by the linear interpolation of the four neighboring pixels, then truncated to integer. (See [5] or [3] for details.) Note that, contrary to the conventional GLDH, α and d are continuous, independent parameters, which makes the proposed regularity measure operational.

The EGLDH is defined as

$$H(k; \alpha, d) = \frac{\left|\{(m, n), (x, y) : m \in I_1, n \in I_2, |I(m, n) - I(x, y)| = k\}\right|}{\left|\{(m, n), (x, y) : m \in I_1, n \in I_2\}\right|}, \tag{2}$$

where the graylevel difference $k \in [0, k_{max}]$, $k_{max} = N_g - 1$, N_g is the number of graylevels, and x, y are given by (1). I_1 and I_2 are the index ranges of the spacing vector origin in the image.

For a discrete set of spacing vectors $\vec{d_{ij}} = (\alpha_i, d_j)$, $i \in [0, N_a - 1]$, $j \in [0, N_d - 1]$, we compute the mean graylevel difference

$$MEAN(i, j) = \frac{1}{k_{max}} \sum_{k=0}^{k_{max}} kH(k; \alpha_i, d_j) \tag{3}$$

Here $\alpha_i = \Delta\alpha \cdot i$, $d_j = \Delta d \cdot j$. The number of angles $N_a = 2\pi/\Delta\alpha$. For a maximum displacement d_{max}, the number of displacements $N_d = d_{max}/\Delta d + 1$. By default, $MEAN(i, 0) = 0$. We use $\Delta d = 1$ with $N_d = d_{max} + 1$.

To cope with varying contrast, $MEAN(i, j)$ is normalized by its maximum value $\max_{ij}\{MEAN(i, j)\}$ so that $0 \leq MEAN(i, j) \leq 1$.

The angular resolution N_a and the maximum spacing d_{max} are two basic parameters of the algorithm. It is assumed that d_{max} extends to at least two periods of the pattern. High angular resolution is necessary for the spacing vector to precisely align with the periodicity vector.

The $MEAN$ feature (3) is related to the autocorrelation function. When viewed as a function of d for a given angle, this feature is called *contrast curve* [1] and denoted by $F(d)$. Figure 2 shows typical contrast curves for patterns with different degrees of regularity. As discussed in [1], a periodic pattern has a contrast curve with deep and periodic minima. Our definition of regularity quantifies this property. It also takes into account that the shape of the period can generally be more complex, with local minima that indicate the presence of a hierarchical structure. The model-based regularity measure [1] cannot cope with hierarchical structures.

2.2 Computational definition of regularity

First, for each angle α_i we compute a regularity value $REG(i)$ called *directional regularity*. Then the *maximal regularity* feature $MAXREG$ is defined as the maximum directional regularity over all angles

$$MAXREG = \max_i\{REG(i)\} \tag{4}$$

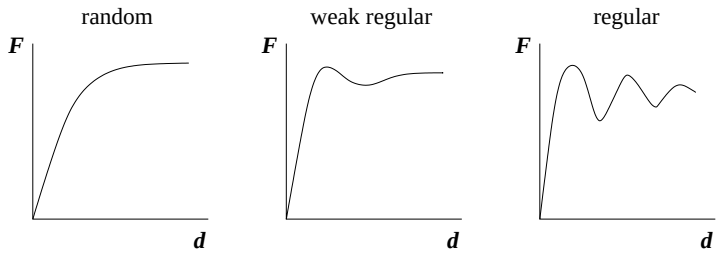

Figure 2: Typical contrast curves of a random, a weak regular and a regular pattern.

Figure 3 illustrates the computation of REG for a periodic contrast curve $F(d)$ having a local minimum within the period. When searching for periodicity, two cases are considered. In the normal case (figure 3a) the depths of the global minima decrease monotonically with d. The special case accounts for possible inhomogeneity of the pattern, when the monotonicity may not hold.

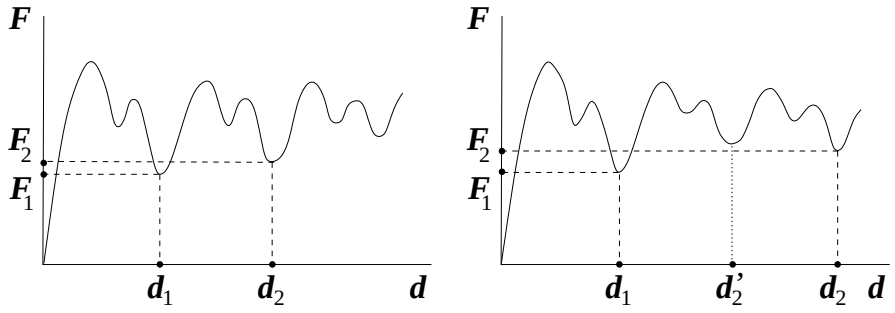

Figure 3: Computing the regularity measure. (a) Normal case. (b) Special case.

The algorithm operates as follows.

Step 1 Apply median filter of width 3 to remove noisy extrema in $F(d)$. Denote the original non-filtered function by $F_0(d)$.

Step 2 Find the extrema of the filtered function $F(d)$, excluding the points $d = 0$ and $d = d_{max}$. (We use the descending component analysis [7].) Denote the number of minima by N_{min}.

Step 3 Select the two lowest minima (d_1, F_1) and (d_2, F_2), $d_1 < d_2$.

Step 4 Set the absolute minimum (d_{am}, F_{am}) at $\min\{F_1, F_2\}$. Rectify F_{am} by searching $F_0(d)$ for an even lower value in the ± 2 point vicinity of d_{am}. Set F_{am} to the lowest value found in this vicinity.

Step 5 Compute the *intensity regularity*

$$REG_{int} = 1 - F_{am} \tag{5}$$

Since $MEAN(i,j)$ has been normalized, $0 \leq REG_{int} \leq 1$. By default, $REG_{int} = 0$ if $N_{min} = 0$.

Step 6 If there is no minimum between d_1 and d_2, compute the *position regularity* as

$$REG_{pos} = 1 - \frac{|d_2 - 2d_1|}{d_2} \tag{6}$$

Otherwise, consider also

$$REG_{pos} = 1 - \frac{|d_2 - 3d_1|}{d_2} \tag{7}$$

and select the larger of (6) and (7). By default, $REG_{pos} = 0$ if $N_{min} < 2$.

Step 7 Compute the directional regularity as

$$REG = (REG_{int} \cdot REG_{pos})^p, \tag{8}$$

where p is a parameter of the algorithm. Currently, we use $p = 2$.

The median filtering removes false extrema, but it also smoothes and shifts the true ones. The correction procedure in step 4 restores the original amplitude. A small shift is accounted for in REG_{int} and is neglected in REG_{pos}. In step 6, two alternatives are considered: d_2 is either the second or the third period. (See figures 3a and 3b, respectively.)

3 Degrees of regularity

In this section we demonstrate that $MAXREG$ is consistent with the visually perceived degree of regularity. Figure 4 shows a collection of patterns whose $MAXREG$ values are given in table 2. These values were computed with the angular resolution $\Delta\alpha = 5°$.

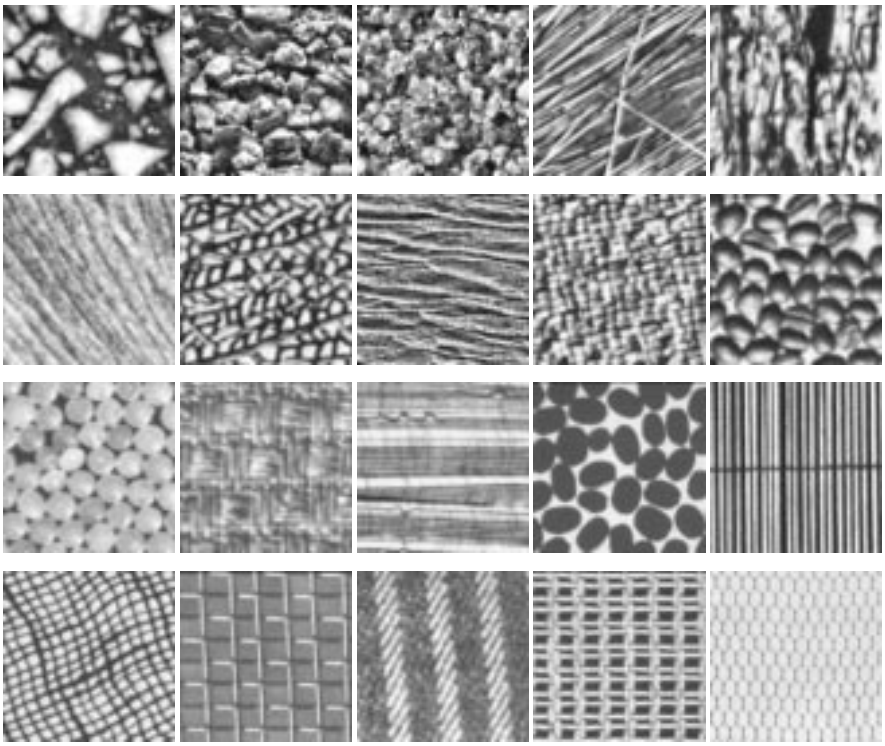

Figure 4: A collection of patterns. The rows show random, low regularity, medium regularity and high regularity patterns, respectively. The regularity value increases in each row from left to right. (See table 2.)

Category	Pattern 1	Pattern 2	Pattern 3	Pattern 4	Pattern 5
Random	0.00	0.07	0.11	0.18	0.22
Low reg.	0.25	0.29	0.32	0.36	0.39
Medium reg.	0.50	0.54	0.58	0.61	0.71
High reg.	0.75	0.82	0.87	0.95	1.00

Table 2: The regularity values of the patterns shown in figure 4.

In figure 4 and table 2, the patterns are grouped in rows as four categories according to their maximal regularity: random $[0, 0.25)$, low regularity $[0.25, 0.50)$, medium regularity $[0.50, 0.75)$ and high regularity $[0.75, 1.00]$. In each row, the value grows from left to right. When evaluating these results, one should keep in mind that $MAXREG$ combines the layout and the intensity regularities. For example, the coffee beans pattern in the third row (backlighting) is considerably more regular than the coffee beans pattern in the second row. The layout regularities of the two patterns are similar, while the elements' intensity in the former pattern is much more regular.

While $MAXREG$ categorizes patterns according to regularity, its discriminating power is limited, as visually very different patterns may have the same maximal regularity value. In particular, this can easily happen to a linear and a tiled pattern whose directional distributions of regularity are completely different. We plan to investigate $REG(i)$ more closely in the near future. However, we envisage that $REG(i)$ will be less invariant and robust than $MAXREG$.

4 Detecting regular structures

The maximal regularity of a flat pattern is invariant under weak perspective, when the size of objects is small compared with the viewing distance. Weak perspective, an approximation widely used in vision research, can be interpreted as an orthographic projection onto the image plane followed by an isotropic scaling [9]. Both transformations preserve periodicity and parallelism. This is sufficient for the stability of the maximal regularity because its components are invariant under linear transformations of intensity due to illumination changes.

Assume that a structure extends in the third dimension as well, but its size in this dimension is small compared to the other two dimensions. Under weak prospective with varying viewing angle and distance, the periodic elements of a regular structure cast shadows that are also periodic. In the visible parts of the pattern, periodicity and parallelism are still preserved, while intensity may change in a non-linear way. Despite this latter circumstance, the maximal regularity tends to be quite stable, as illustrated in the introduction of this paper.

We used this property of $MAXREG$ for invariant detection of regular structures in the RADIUS images [10]. These images contain two or more non-flat regular structures viewed under weak perspective and varying illumination. The $MAXREG$ feature was implemented in a flexible *regularity filter* selective to the local regularity computed in a sliding window. The implementation is based on the previously developed running filter version of the $MEAN$ feature (3). The $MEAN$ filter is described in [2, 3]. The extension of the $MEAN$ filter to $MAXREG$ is straightforward.

The size of the filter window is related to the maximum displacement d_{max}. By changing d_{max}, one can tune the structure detector to short- or long-period regularity, as demonstrated in figure 5. When d_{max} is set so as to exceed two periods of the long-period, linear roof structure, this structure appears in the filtered image. Note that the first image contains a poorly visible long-period structure in the bottom-left corner.

The angular resolution of the structure detector was set to $\Delta\alpha = 15^\circ$. Lower resolution, e.g., the one provided by the conventional co-occurrence, is not sufficient for stable performance under varying viewing conditions.

Earlier, we applied the $MEAN$ feature of the EGLDH to precise anisotropy and orientation analysis of patterns [5, 3]. By combining this approach with the maximal regularity filtering, one can detect structures of given orientation.

5 Detecting structural defects

Instead of detecting locations of high regularity, one can use the regularity filter to indicate locations of low regularity in regular structures. Such locations are typically *structural de-*

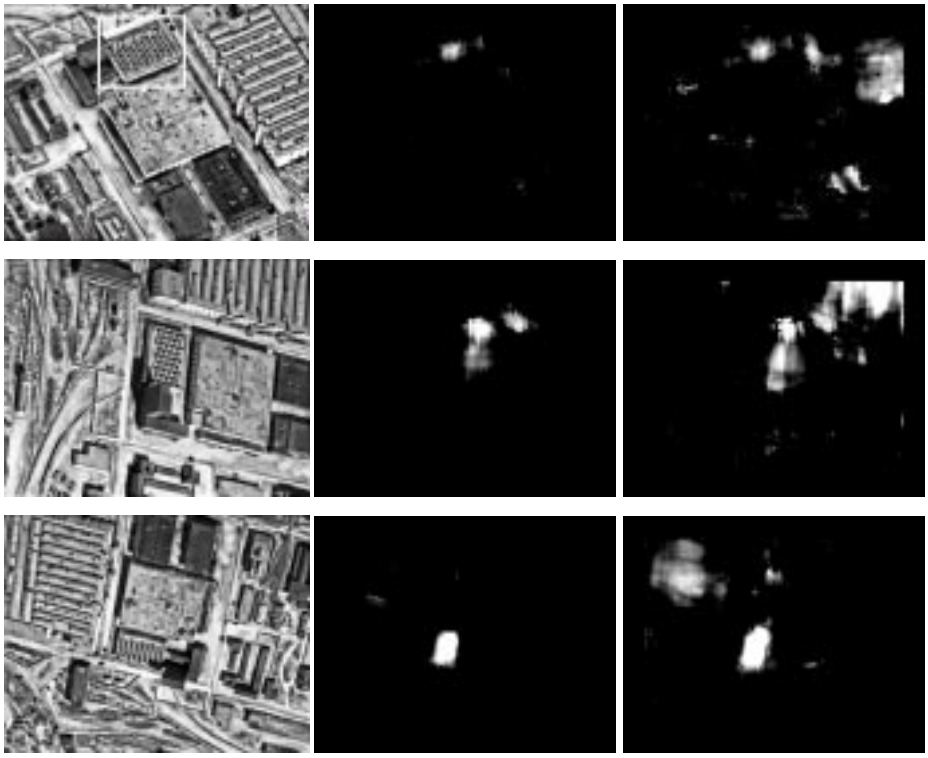

Figure 5: Detecting regular structures in model board images. In each row, a model board image and the enhanced results of short- and long-range filtering are displayed. The box in the first image indicates the structure whose different views are shown in figure 1.

fects whose detection is of importance in industrial texture inspection and some scientific applications.

Recently, we proposed a related, novel method for this task [4]. Implemented as the running filter, the algorithm [4] matches $MEAN(i,j)$ of the sliding window against the pre-computed $MEAN(i,j)$ of a reference (ideal) patch. Since the basic texture may have tolerable variations, the matching is adaptive, with the tolerances in the local orientation and size being specified by the user. In the resulting filtered image, a blob detector locates defects as areas of large structural deviation from the reference pattern. (See [4] for details.)

Alternatively, the same blob detector can be applied to regularity-filtered images, as shown in figure 6. In this new approach, neither reference patch nor explicit orientation or size tolerances are to be given: a regularity variation threshold is only specified. To demonstrate the robustness of this method, the last pattern is a rotated, skewed and tilted version of the previous one.

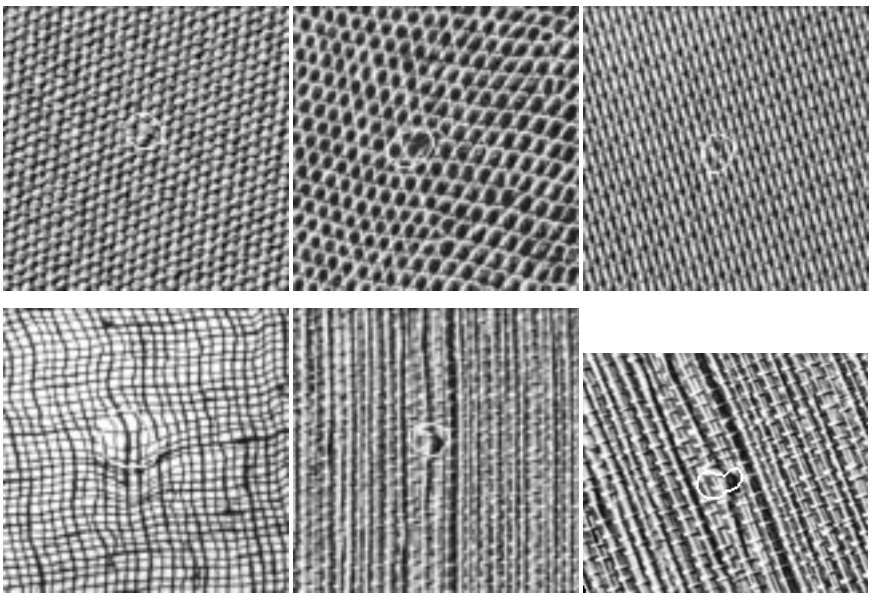

Figure 6: Regularity-based detection of structural defects.

6 Conclusion

We have discussed the role of pattern regularity in machine vision and introduced a new, highly invariant maximal regularity feature. Pilot examples of its application to a number of problems have been shown. Currently, the proposed method is limited by its computational cost which is still high despite the run filtering implementation: regularity filtering of an average size image takes several minutes on an advanced PC. More research and testing are needed to justify the algorithms and to systematically evaluate their performance, especially as far as 3D invariance, generality, scalability and robustness are concerned. We plan to continue the development of the approach and to use it in different applications, including retrieval of structures for image database management.

Acknowledgments. This work is supported by grants OTKA T026592 and INCO-COPERNICUS CT96-0742. The author thanks Robert Haralick for providing CD's with the RADIUS Model Board Imagery Database.

References

[1] D. Chetverikov. Measuring the degree of texture regularity. In *Proc. International Conf. on Pattern Recognition*, pages 80–82, 1984.

[2] D. Chetverikov. Structural filtering with texture feature based interaction maps: Fast algorithm and applications. In *Proc. International Conf. on Pattern Recognition*, pages 795–799. Vol.II, 1996.

[3] D. Chetverikov. Texture analysis using feature based pairwise interaction maps. *Pattern Recognition*, Special Issue on Color and Texture, 1998, in press.

[4] D. Chetverikov and K. Gede. Textures and structural defects. In G.Sommer et.al., editor, *Computer Analysis of Images and Patterns*, volume Lecture Notes in Computer Science, vol.1296, pages 167–174. Springer Verlag, 1997.

[5] D. Chetverikov and R.M. Haralick. Texture anisotropy, symmetry, regularity: Recovering structure from interaction maps. In *Proc. British Machine Vision Conference*, pages 57–66, 1995.

[6] F. D'Astous and M.E. Jernigan. Texture discrimination based on detailed measures of the power spectrum. In *Proc. International Conf. on Pattern Recognition*, pages 83–86, 1984.

[7] R. M. Haralick and L. G. Shapiro. *Computer and Robot Vision*, volume I-II. Addison-Wesley, 1992-1993.

[8] F. Liu and R.W. Picard. Periodicity, Directionality, and Randomness: Wold Features for Image Modeling and Retrieval. *IEEE Trans. Pattern Analysis and Machine Intelligence*, 18:722–733, 1996.

[9] J.L. Mundy and A. Zisserman. Projective geometry in machine vision. In J.L. Mundy and A. Zisserman, editors, *Geometric Invariance in Computer Vision*, pages 463–534. MIT Press, 1992.

[10] University of Washington. RADIUS Model Board Imagery Database I,II. *Reference Manual*, 1996.

[11] A.R. Rao and G.L. Lohse. Identifying high level features of texture perception. *CVGIP: Image Processing*, 55:218–233, 1993.

[12] H. Tamura, S. Mori, and T. Yamawaki. Textural features corresponding to visual perception. *IEEE Trans. Systems, Man, and Cybernetics*, 8:460–473, 1978.

[13] S.W. Zucker and Terzopoulos. Finding structure in co-occurence matrices for texture analysis. *Comp. Graph. and Image Proc.*, 12:1286–1308, 1980.